

1N-24
1701
p20
NASA Technical Memorandum 103669

Probabilistic Micromechanics³ and Macromechanics of Polymer Matrix Composites

(NASA-TM-103669) PROBABILISTIC
MICROMECHANICS AND MACROMECHANICS OF POLYMER
MATRIX COMPOSITES (NASA) 20 p CSCL 11D

N91-19236

Unclass

63/24 0001701

G.T. Mase
GMI Engineering and Management Institute
Flint, Michigan

and

P.L.N. Murthy and C.C. Chamis
Lewis Research Center
Cleveland, Ohio

Prepared for the
14th Annual Energy-sources Technology Conference and Exhibition
sponsored by the American Society of Mechanical Engineers
Houston, Texas, January 20-24, 1991

NASA

1. The first part of the document is a title page.

2. The second part of the document is a table of contents.

3. The third part of the document is a list of figures.

4. The fourth part of the document is a list of tables.

5. The fifth part of the document is a list of references.

6. The sixth part of the document is a list of appendices.

7. The seventh part of the document is a list of footnotes.

8. The eighth part of the document is a list of glossary terms.

9. The ninth part of the document is a list of index terms.



PROBABILISTIC MICROMECHANICS AND MACROMECHANICS OF POLYMER MATRIX COMPOSITES

G.T. Mase*
GMI Engineering and Management Institute
Flint, MI 48504-4898

and

P.L.N. Murthy† and C.C. Chamis‡
NASA Lewis Research Center
Cleveland, Ohio 44135

ABSTRACT

A probabilistic evaluation of an eight-ply graphite/epoxy quasi-isotropic laminate was completed using the Integrated Composite Analyzer (ICAN) in conjunction with Monte Carlo simulation and Fast Probability Integration (FPI) techniques. Probabilistic input included fiber and matrix properties, fiber misalignment, fiber volume ratio, void volume ratio, ply thickness and ply layup angle. Cumulative distribution functions (CDF's) for select laminate properties are given. To reduce number of simulations, a Fast Probability Integration (FPI) technique was used to generate CDF's for the select properties in the absence of fiber misalignment. These CDF's were compared to a second Monte Carlo simulation done without fiber misalignment effects. It is found that FPI requires a substantially less number of simulations to obtain the cumulative distribution functions as opposed to Monte Carlo Simulation techniques. Furthermore, FPI provides valuable information regarding the sensitivities of composite properties to the constituent properties, fiber volume ratio and void volume ratio.

SYMBOLS

$E_{c_{xx}}$	composite elastic modulus (Mpsi) about structural axes
$E_{f11}, E_{f22}, G_{f12}$	fiber elastic moduli about material axes
E_m, G_m	matrix elastic moduli
$F(x), p_f$	cumulative distribution function
$f(x)$	probability density function
$f_{\underline{x}}(\underline{X})$	joint probability density function
$G_{c_{xy}}$	composite shear modulus (Mpsi) about structural axes
g	FPI limit state function

*Assistant Professor, Department of Mechanical Engineering.

†Aerospace Research Engineer, Structures Division.

‡Senior Aerospace Scientist, Structures Division.

g_1	linear approximation of g
g_2	incomplete quadratic approximation of g
k_f, k_m, k_v	fiber volume fraction, matrix volume fraction, void volume fraction
u	standardized normal deviate
x	uniform deviate
y	normal, Weibull or gamma deviate
Z	FPI response function
α, β	Weibull distribution parameters
α_{cxx}	composite thermal expansion coefficient (ppm/°F) about structural axes
$\Gamma(x)$	gamma function
λ, κ	gamma distribution parameters
μ, σ	normal distribution parameters
ν_{f12}, ν_m	fiber and matrix Poisson's ratios

INTRODUCTION

The properties of the polymer matrix composites display considerable scatter because of the variation inherent in the properties of constituent materials. Distinct distributions to describe the effects of scatter on composite properties facilitate the composite mechanics calculations. For example composite strength is often examined probabilistically by assuming that the ply failure strength has a specific distribution (usually Weibull) which is then used in a laminate failure criterion (1). Analysis of this type has the shortcoming that different failure mechanisms occurring at a lower level, that is, at the fiber and matrix level are not directly accounted for when the ply failure stress is the primitive random variable.

A better approach to quantify the uncertainties in the behavior of composites would be to account for the variations in the properties starting from the constituent (fiber and matrix) level and integrating progressively to arrive at the global or composite level behavior. Typically, these uncertainties may occur at the constituent level (fiber and matrix properties), at the ply level (fiber volume ratio, void volume ratio, etc.) and the composite level (ply angle and lay-up). In this paper, a computational simulation technique is described which accounts for uncertainties at various levels to predict the behavior of a quasi-isotropic graphite/epoxy (0/45/90-45)_s laminate.

MICROMECHANICAL AND MACROMECHANICAL UNCERTAINTIES

Uncertainties at the Micromechanics Level

To account for uncertainties at all levels of a composite, one has to start with uncertainties at the fiber and matrix level and use composite mechanics to obtain laminate level response. In the present effort the composite mechanics available in ICAN (2) is utilized to obtain the ply/laminate level response. At the micromechanics level 29 parameters (the constituent properties) are required by ICAN as input (2) (schematic Fig. 1). In addition three fabrication process variables (Table II) are needed to compute ply properties. For the most part, these properties were considered to be normally distributed about some mean value. However, the fiber and matrix strengths were taken to be distributed as a Weibull distribution which is widely accepted for strength distributions because of its dispersed left tail and sharp right tail which represents experimental data well.

The distribution types and parameters for the fiber and matrix constituent material properties are given in Table I. Using the Monte Carlo simulation, these distribution types reproduce histograms (frequency of occurrence) plots as shown in Fig. 2 for fiber longitudinal modulus and in Fig. 3 for fiber longitudinal strength. It would require testing of 1000 specimens to generate them experimentally (a rather expensive and time consuming task). It is worth noting that for the Weibull distribution the mean is not parameter 1 nor is the variance parameter 2. In this case the probability density function, mean and variances are given by (3).

$$f(y) = \frac{\beta}{\lambda} \left(\frac{y}{\lambda}\right)^{\beta-1} e^{-\left(\frac{y}{\lambda}\right)^{\beta}}$$

where

$$\lambda^{\beta} = \frac{1}{\alpha} \quad (1)$$

$$\text{Mean} = \alpha^{-\frac{1}{\beta}} \Gamma\left(1 + \frac{1}{\beta}\right), \quad \text{Variance} = \alpha^{-\frac{2}{\beta}} \left[\Gamma\left(1 + \frac{2}{\beta}\right) - \Gamma^2\left(1 + \frac{1}{\beta}\right) \right] \quad (2)$$

Uncertainties at the Ply Level

The next level of uncertainties enters at the ply level. A typical graphite fiber has a nominal diameter of 0.0003 in. which means that a single ply contains many fibers through the thickness. If an eight-ply graphite/epoxy composite is considered with a nominal thickness of 0.04 in. each ply will be approximately 0.005 in. thick. Taking into account an interfiber spacing of 0.00005 (for a ply with fiber volume ratio 0.6) in. there are about 15 fibers through the thickness of each ply. All of these fibers will have a certain amount of misalignment (random orientation). To account for this randomness in probabilistic micromechanics, linear laminate theory is used where each ply is broken down (substructured) into 15 subplies (2). Each of these subplies

was assumed to be normally distributed about the fiber direction with fiber orientations lying within $\pm 5^\circ$ of the 0° -ply direction. The properties of the constituents are assumed to be the same in the subplies within each ply. The fiber volume and ply thickness were represented as normally distributed while the void volume was represented as a gamma distribution. A gamma distribution was the proper choice for the void volume ratio because there is no probability for zero void volume and a bias towards higher void volumes.

As was the case for the Weibull distribution, the parameters given for the gamma distribution do not directly represent the mean and variance of the distribution. The probability density function, mean and variance for the gamma function are given by (3).

$$f(y) = \frac{\lambda^k}{\Gamma(k)} e^{-\lambda y} y^{k-1} \quad (3)$$

$$\text{Mean} = \frac{k}{\lambda}, \text{ Variance} = \frac{k}{\lambda^2} \quad (4)$$

The ply level distribution parameters are given in Table II.

Uncertainties at the Laminate Level

The uncertainty considered at the laminate level was that of ply orientation and thickness. Each ply in the $(0/45/90/-45)_s$ was given a normal distribution with a 3.33° standard deviation about the deterministic angle (Table III).

MONTE CARLO SIMULATION

Given the distributions of Tables I, II and III for fiber and matrix properties, ply and laminate inputs, the uncertainties in the composite properties need to be quantified with appropriate cumulative distribution functions (CDF's). One approach to achieve this is to use a Monte Carlo Simulation technique. The first step in this process involves running ICAN with randomly selected input variables from the predetermined probability distribution functions many times. The output comprising of the composite properties is saved. The second step consists of processing the various property output data to compute the desired CDF. An obvious disadvantage of such an approach is the enormous number of output sets that must be obtained to get reasonable accuracy in the output CDF's.

Generation of Normal Distributions

In order to generate the input distributions, a uniform deviate (random number between 0 and 1) must first be generated. Rather than use a machine routine to generate the random number, a portable (machine independent) uniform deviate routine from Press et al. (4) was used which was based on a three linear congruential generator method. This routine also had the advantage of being able to reinitialize the random sequence.

The uniform deviate was used to generate a normal deviate by the Box-Muller method (4). With the aid of the normal distribution $f(y)$ given by

$$f(y)dy = \frac{1}{\sqrt{2\pi}} e^{-\frac{y^2}{2}} dy \quad (5)$$

and the transformation between uniform deviates x_1, x_2 and the variables y_1, y_2 given by

$$y_1 = \sqrt{-2 \ln x_1} \cos 2\pi x_2, \quad y_2 = \sqrt{-2 \ln x_1} \sin 2\pi x_2, \quad (6)$$

the inverse transformation can be written as

$$x_1 = e^{-\frac{y_1^2 + y_2^2}{2}}, \quad x_2 = \frac{1}{2\pi} \arctan \frac{y_2}{y_1}. \quad (7)$$

The Jacobian of this transformation is

$$\frac{\partial(x_1, x_2)}{\partial(y_1, y_2)} = - \begin{bmatrix} \frac{1}{\sqrt{2\pi}} e^{-\frac{y_1^2}{2}} \\ \frac{1}{\sqrt{2\pi}} e^{-\frac{y_2^2}{2}} \end{bmatrix} \begin{bmatrix} \frac{y_1^2}{2} \\ \frac{y_2^2}{2} \end{bmatrix} \quad (8)$$

which shows that each y is distributed normally. This shows that Eq. (6) leads to an explicit formula for calculating a normal deviate.

Generation of Weibull Distribution

To generate a Weibull distribution from a uniform deviate one can integrate the probability density function and then solve for the Weibull deviate. This gives

$$y = \beta [-\ln(1 - x)]^{\frac{1}{\alpha}} \quad (9)$$

as a point from the Weibull distribution where x is a uniform deviate.

Generation of Gamma Distribution

To generate a deviate from a gamma distribution, a uniform deviate, x , was taken and then the zero of the function

$$w(y) = \sum_{k=0}^{\infty} \frac{\lambda^k}{\Gamma(k)} e^{-\lambda y} y^{k-1} dx - x \quad (10)$$

was found. This was numerically inefficient because it involved numerical integration and root finding by the bisection method, but the program ran with sufficient speed to overlook this fact.

The program ICAN was modified so that the properties shown in Tables I, II and III were given a value from their respective distributions. Output for the layer and composite properties were saved for 200 samples. While 200 samples is probably not enough to converge to the actual CDF, the results do show a good qualitative trend. The cumulative distribution functions were constructed from these samples for three typical composite properties. The selected composite properties are the composite longitudinal modulus E_{CXX} , the composite compressive strength S_{CXXC} , and the composite thermal expansion coefficient α_{CXX} . These CDF's are shown in Figs. 4 to 6. By its symmetry, the CDF of E_{CXX} appears to be normally distributed while S_{CXXC} exhibits a Weibull shape (5).

FPI SIMULATION

An alternative approach to obtain the required cumulative distribution functions is to use Fast Probability Integration (FPI) program (6). FPI helps generate the required CDF's quicker with reasonable accuracy and a lot less number of sample output data. Also, it generates more information than what can be expected from a Monte Carlo simulation. The additional information that FPI offers is the output variable sensitivity information based on the probabilistic inputs.

A brief overview of FPI is given below. The reader is advised to refer to (6) for a detailed discussion.

Consider a response function

$$Z(\underline{X}) = Z(X_1, X_2, \dots, X_n) \quad (11)$$

where X_1, \dots, X_n are random variables. Also, define the function

$$g = Z(\underline{X}) - Z_0 = 0 \quad (12)$$

as the limit state with Z_0 a real value of $Z(\underline{X})$. The CDF of Z at Z_0 is equal to the probability that $[g \leq 0]$. If the probability of a desired output, p_f , is defined by

$$p_f = P[g < 0] \quad (13)$$

an exact solution of p_f can be obtained from

$$p_f = \dots \int_{\Omega} f_{\underline{X}}(\underline{X}) d\underline{X} \quad (14)$$

where $f_X(\underline{X})$ is the joint probability density function and Ω is the region defined by $[g \leq 0]$.

The evaluation of the preceding integral is often intractable and this leads to the need for an approximate method of evaluation p_f . In doing this, FPI approximates the function g using a Taylor's series expansion as a linear

$$g_1(\underline{u}) = a_0 + \sum_{i=1}^n a_i (u_i - u_i^*) \quad (15)$$

or incomplete quadratic

$$g_2(\underline{u}) = a_0 + \sum_{i=1}^n a_i (u_i - u_i^*) + \sum_{i=1}^n b_i (u_i - u_i^*)^2 \quad (16)$$

function where u_i^* is the most probable point (6) of the random variable u_i . Note that the random variables \underline{X} have been replaced by standardized normal variables \underline{u} . The coefficients of these expansions are obtained numerically and then the probability $P[g < 0]$ is computed.

Because of the approximate form of the g -function, FPI requires at least $n+1$ or $2n+1$ data sets to evaluate the linear or quadratic g -function coefficients a_0 , a_i , and b_i from which the probability is found. In the present effort only the ply level variations in the properties (29), fiber volume ratio and void volume ratio are considered as random variables. This means that at least 32 (29 constituent properties, fiber volume ratio, void volume ratio +1) ICAN runs are needed for the linear approximation and 63 for the quadratic approximation. A typical data set to FPI consisted of ICAN run with one perturbed independent variable while all others remaining at mean value. For the linear case, the variable was perturbed one standard deviation from its mean value. In the quadratic case, the independent variables were perturbed twice, one standard deviation each, on both sides of the mean value.

Three typical composite properties E_{CXX} , G_{CXY} , and α_{CXX} were chosen as the output variables for the study. Since the goal was to have a minimum number of ICAN runs, the CDF of E_{CXX} was calculated using 32 data sets with linear FPI analysis and 125 data sets with quadratic analysis. With these two cases, the CDF's computed by FPI lay on top of each other indicating that 32 data sets will give a good approximation for the CDF of E_{CXX} .

To identify the computational savings that FPI has over a Monte Carlo simulation, the CDF's for E_{CXX} , G_{CXY} , and α_{CXX} were compared for a 32 sample FPI case with a 31 and 90 sample Monte Carlo simulation (Figs. 7 to 9). It appears that the Monte Carlo simulation is converging to the FPI simulation, but the FPI simulation only needed 32 samples.

FPI Sensitivity Output

As was previously mentioned, one advantage of FPI is the sensitivity data that it produces. Before the actual sensitivity numbers are given for the composite modulus E_{CXX} , it will be helpful to examine how this quantity is calculated by ICAN.

The modulus E_{CXX} is the (1,1) entry of the matrix (2)

$$[E_C] = \frac{1}{t_c} \left[\sum_{i=1}^{N_l} (Z_{li+1} - Z_{li}) ([R_l]^T [E_l] [R_l]) \right]_i \quad (17)$$

where t_c is the thickness of the composite, Z_{li} is the distance from the bottom of the composite to the ply, $[R_l]$ is rotation matrix which is a function of the ply angle, $[E_l]$ is the matrix of the layer elastic constants, distortional energy coefficient. To calculate the ply elastic moduli matrix, $[E_l]$, the components are calculated from primitive variables E_{f11} , E_{f22} , E_m , G_{f12} , G_{f23} , G_m , k_f , k_m , ν_{f12} , and ν_m (2). So in the case of no ply substructuring or ply angle variation, the composite modulus should be a function of only these 10 primitive variables. It is noted that k_m is calculated by

$$k_m = 1 - k_f - k_v \quad (18)$$

and is not listed as a primitive variable. Thus k_v will be used instead of k_m in the sensitivity analysis.

For the input random variables given previously, FPI calculated a mean E_{CXX} of $\mu = 5.744$ Mpsi with a standard deviation of $\sigma = 0.363$ Mpsi. The sensitivities at $\pm 0.3\sigma$ are given in Table IV. As would be expected, the most sensitive primitive variables are the fiber modulus E_{f11} and the fiber volume ratio k_f . Primitive variable G_{f23} has a zero sensitivity which is consistent with the definition of E_{CXX} given in matrix Eq. (17).

CONCLUSIONS

A probabilistic evaluation of an eight-ply quasi-isotropic graphite/epoxy [0/45/90/-45]_s laminate was completed using two approaches. The first approach was to use a Monte Carlo simulation technique. The second approach was to use fast probability integration technique (FPI). Probabilistic inputs for this study included constituent micromechanical properties, fiber misalignment within a ply, fiber volume fraction, void volume percent and ply angle misalignment for the laminate.

It was demonstrated that the use of the FPI program can greatly reduce the computations needed to generate composite CDF's. FPI was demonstrated by generating CDF's for E_{CXX} , G_{CXY} and α_{CXX} for a graphite/epoxy [0/45/90/-45]_s composite in the absence of fiber misalignment.

The results of this investigation indicate that an integrated program combining ICAN and FPI is feasible. Such an integrated program offers the potential for a computational efficient probabilistic composite mechanics methodology.

REFERENCES

1. Duva, J.M., Lang, E.J., Mirzadeh, F., and Herakovich, C.T., 1990, "A Probabilistic Perspective on the Failure of Composite Laminae," presented at the XI U.S. National Congress of Applied Mechanics, Tucson, AZ, May.
2. Murthy, P.L.N. and Chamis, C.C., 1986, "Integrated Composite Analyzer (ICAN), Users and Programmers Manual," NASA TP-2515.
3. Mood, A.M., Graybill, F.A., and Boes, D.C., 1974, Introduction to the Theory of Statistics, 3rd Edition, McGraw-Hill, New York, NY.
4. Press, W.H., Flannery, B.P., Teukolsky, S.A., and Vetterling, W.T., 1986, Numerical Recipes, Cambridge University Press, Cambridge, U.K.
5. Stock, T.A., 1987, Probabilistic Fiber Composite Micromechanics, MS Thesis, Cleveland State University, Cleveland, OH.
6. Probabilistic Structural Analysis Methods (PSAM) for Select Space Propulsion Systems Components, NESSUS/FPI Theoretical Manual, 1989, Southwest Research Institute, NASA Contract NAS3-24389, Dec.

TABLE I. - CONSTITUENT INPUT DISTRIBUTION PARAMETERS FOR ICAN

	Distribution		Parameter 1	Parameter 2
	Units	Type		
E _{f11}	Mpsi	Normal	$\mu = 31.0$	$\sigma = 1.5$
E _{f22}	Mpsi	↓	$\mu = 2.0$	$\sigma = 0.10$
G _{f12}	Mpsi	↓	$\mu = 2.0$	$\sigma = 0.10$
G _{f23}	Mpsi	↓	$\mu = 1.0$	$\sigma = 0.05$
ν_{f12}	in./in.	↓	$\mu = 0.20$	$\sigma = 0.01$
ν_{f23}	in./in.	↓	$\mu = 0.25$	↓
α_{f11}	ppm/°F	↓	$\mu = 0.2$	↓
α_{f22}	ppm/°F	↓	$\mu = 0.2$	↓
ρ_f	lb/in. ³	↓	$\mu = 0.063$	$\sigma = 0.003$
N _f	-----	Fixed	$\mu = 10\ 000$	$\sigma = 0$
d _f	in.	Normal	$\mu = 0.003$	$\sigma = 0.00015$
C _f	BTU/lb	↓	$\mu = 0.20$	$\sigma = 0.01$
K _{f11}	(a)	↓	$\mu = 580$	$\sigma = 2.9$
K _{f22}	(a)	↓	$\mu = 58$	$\sigma = 2.9$
K _{f33}	(a)	↓	$\mu = 58$	$\sigma = 2.9$
S _{fT}	ksi	Weibull	$\beta = 400$	$\sigma = 40$
S _{fC}	ksi	Weibull	$\beta = 400$	$\sigma = 40$
E _m	Mpsi	Normal	$\mu = 0.500$	$\sigma = 0.025$
G _m	Mpsi	(b)	-----	-----
ν_m	in./in.	Normal	$\mu = 0.35$	$\sigma = 0.035$
α_m	ppm/°F	↓	$\mu = 36$	$\sigma = 4$
ρ_m	lb/in. ³	↓	$\mu = 0.0443$	$\sigma = 0.0022$
C _m	BTU/lb	↓	$\mu = 0.25$	$\sigma = 0.0125$
K _m	(a)	↓	$\mu = 1.25$	$\sigma = 0.06$
S _{mT}	ksi	Weibull	$\mu = 15$	$\alpha = 5$
S _{mC}	ksi	Weibull	$\mu = 35$	$\alpha = 20$
S _{mS}	ksi	Weibull	$\mu = 13$	$\alpha = 7$
β_m	in./in. 1% moisture	Normal	$\mu = 0.004$	$\sigma = 0.0002$
D _m	in. ² /sec	Normal	$\mu = 0.002$	$\sigma = 0.0001$

a \equiv BTU · in./hr/ft²/°F.

b G_m is calculated using E_m and ν_m , and isotropy.

TABLE II. - PLY INPUT DISTRIBUTION PARAMETERS FOR ICAN

	Units	Distribution type	Parameter 1	Parameter 2
k_f	Percent	Normal	$\mu = 60$	$\sigma = 3$
k_v	Percent	Gamma	$\lambda = 2$	$k = 6$
θ_f	Degrees	Normal	$\mu = 0$	$\sigma = 3.33$

TABLE III. - LAMINATE INPUT DISTRIBUTION PARAMETERS FOR ICAN

	Units	Distribution type	Parameter 1	Parameter 2
θ_l	Degrees	Normal	$\mu = 0$	$\sigma = 3.33$
t_l	Inches	Normal	$\mu = t_0$	$\sigma = 0.05t_0$

TABLE IV. - NONZERO SENSITIVITY

PARAMETERS FOR E_{cxx} FROMFPI AT $\pm 0.3\sigma$ AWAY FROMMEAN OF $\mu = 5.744$ MPsi

Primitive variable	Sensitivity parameter
k_f	0.778
E_{f11}	.624
E_{f22}	.260
G_{f12}	.130
G_m	.060
E_m	.036
G_{f23}	.0
ν_{f12}	↓
ν_{f12}	
ν_m	
k_v	

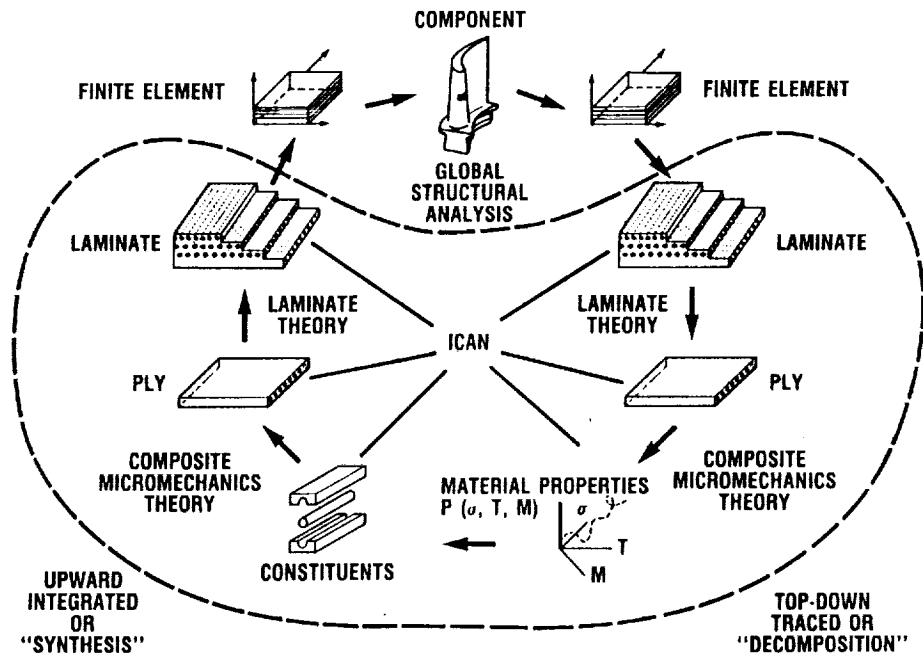


Figure 1. – Integrated composite micro- and macromechanics analysis embedded in the computer code ICAN.

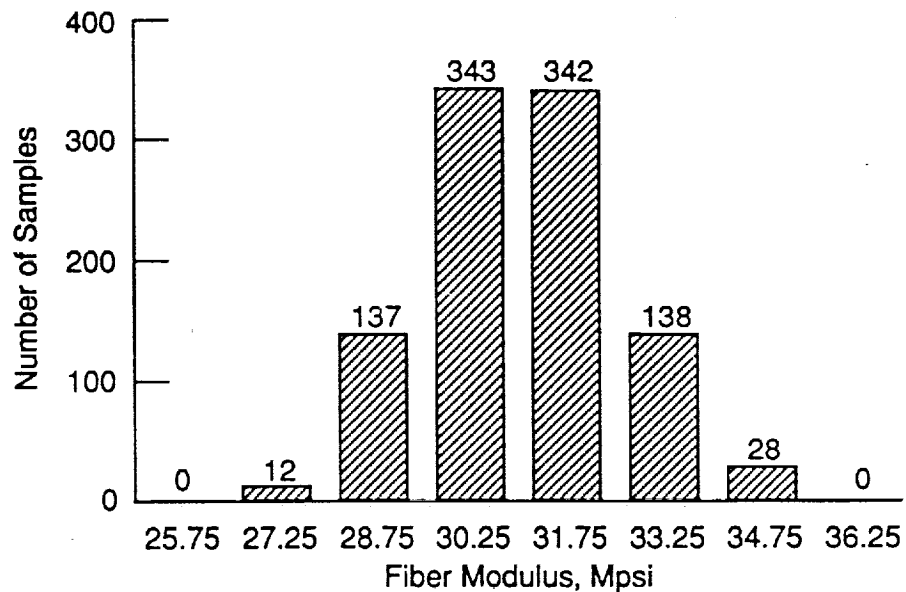


Figure 2. – Monte Carlo simulation (1000 samples) of fiber longitudinal modulus from a normal distribution.

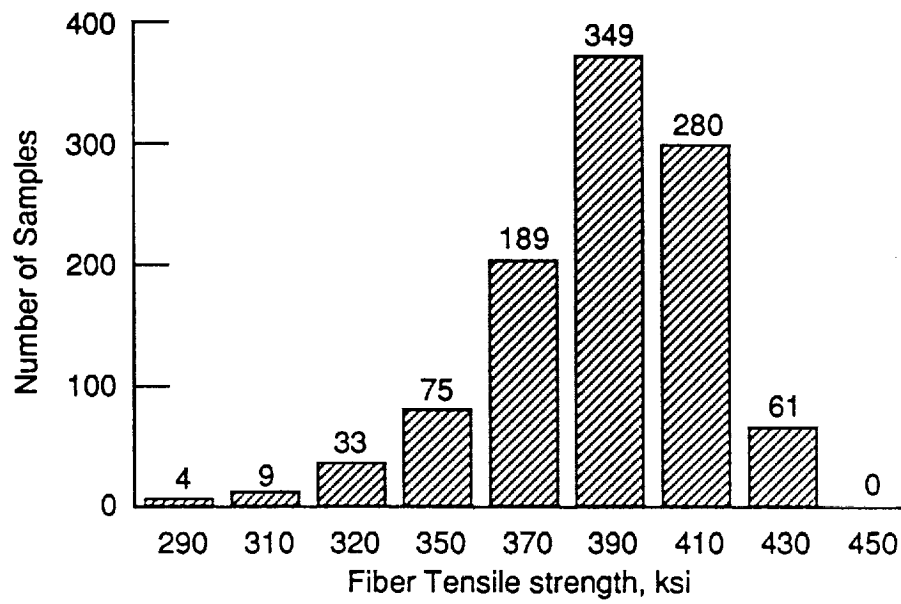


Figure 3. – Monte Carlo simulation (1000 samples) of fiber longitudinal strength from a Weibull distribution.

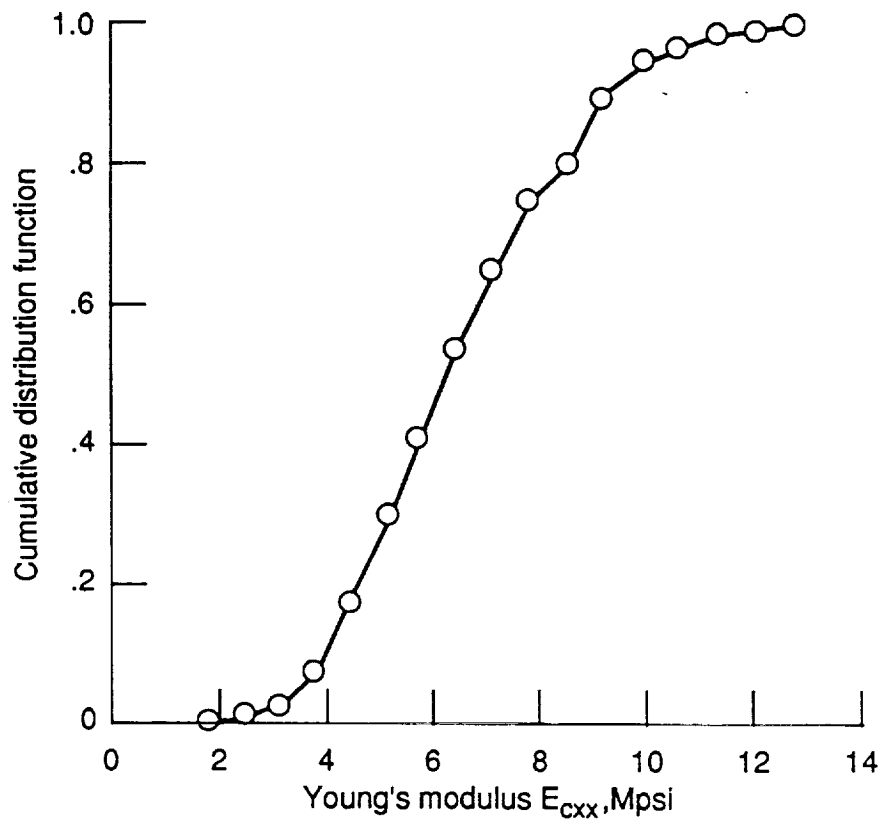


Figure 4. – Cumulative distribution function for composite $([0/45/90/-45]_s)$ modulus E_{cxx} from Monte Carlo simulation (200 samples) which includes ply substructuring effects.

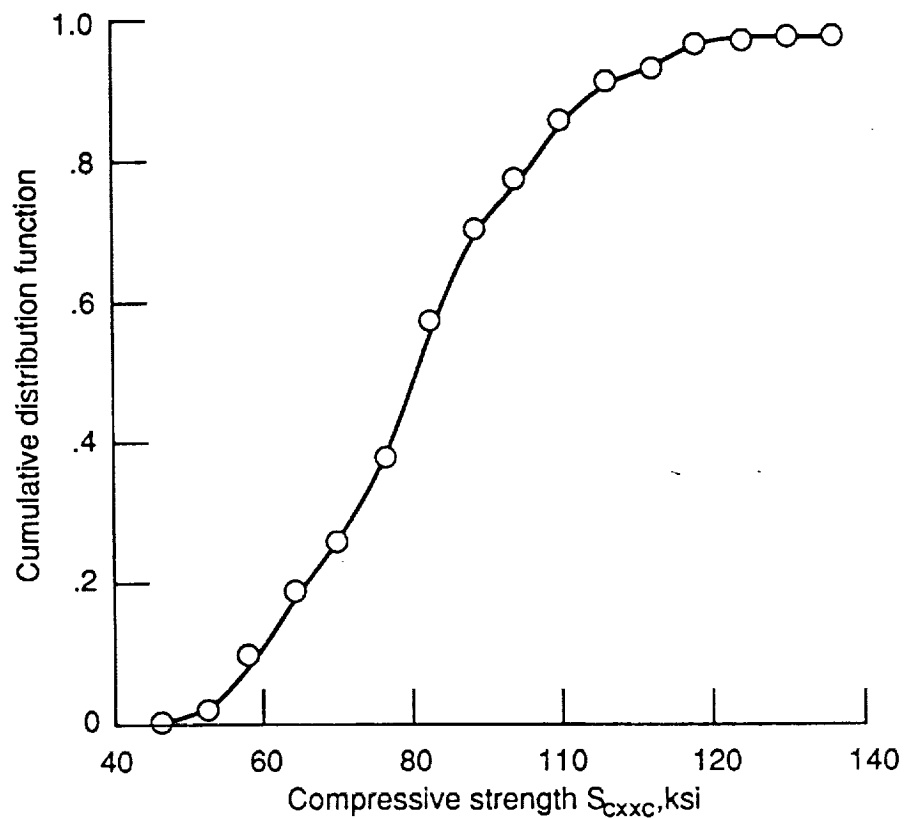


Figure 5. – Cumulative distribution function for composite $([0/45/90/-45]_s)$ modulus S_{cxc} from Monte Carlo simulation (200 samples) which includes ply substructuring effects.

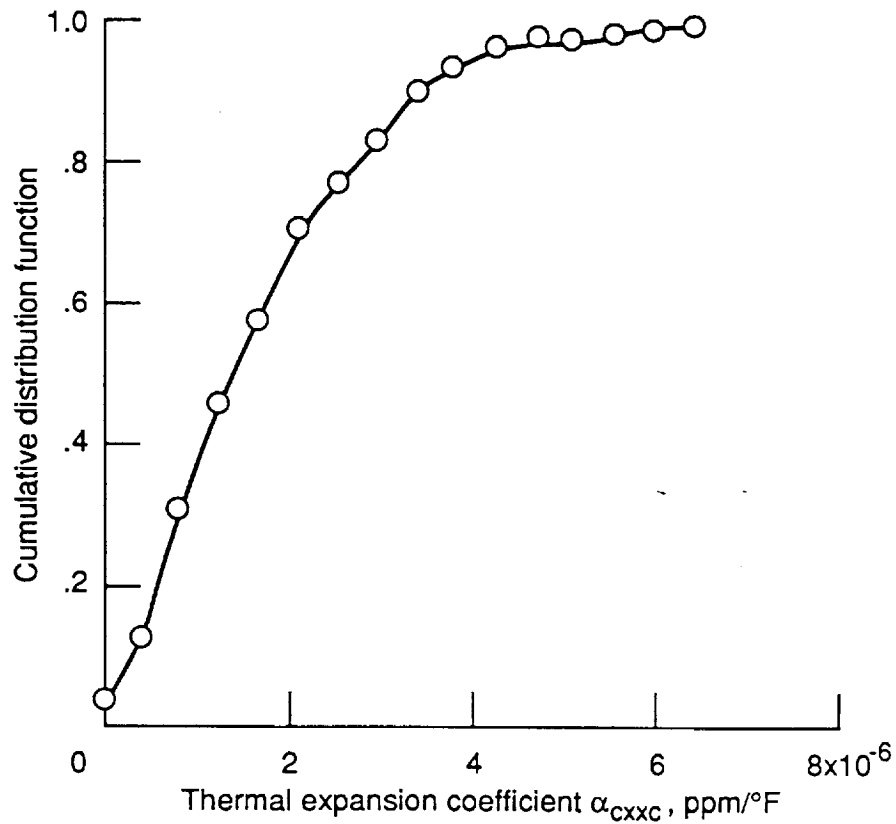


Figure 6. – Cumulative distribution function for composite $[\text{o}/45/90/-45]_s$ thermal expansion coefficient α from Monte Carlo simulation (200 samples) which includes ply substructuring effects.

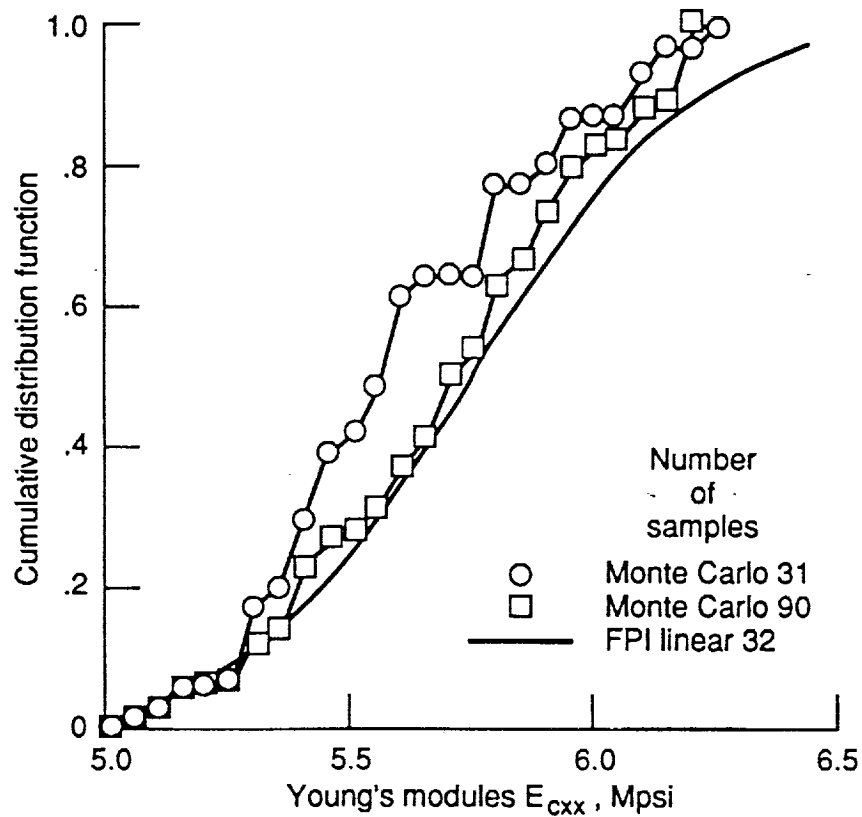


Figure 7. – Cumulative distribution function for composite $([0/45/90/-45]_s)$ modulus E_{cxx} simulation with Monte Carlo (no ply substructuring) and Fast Probability Integration (FPI).

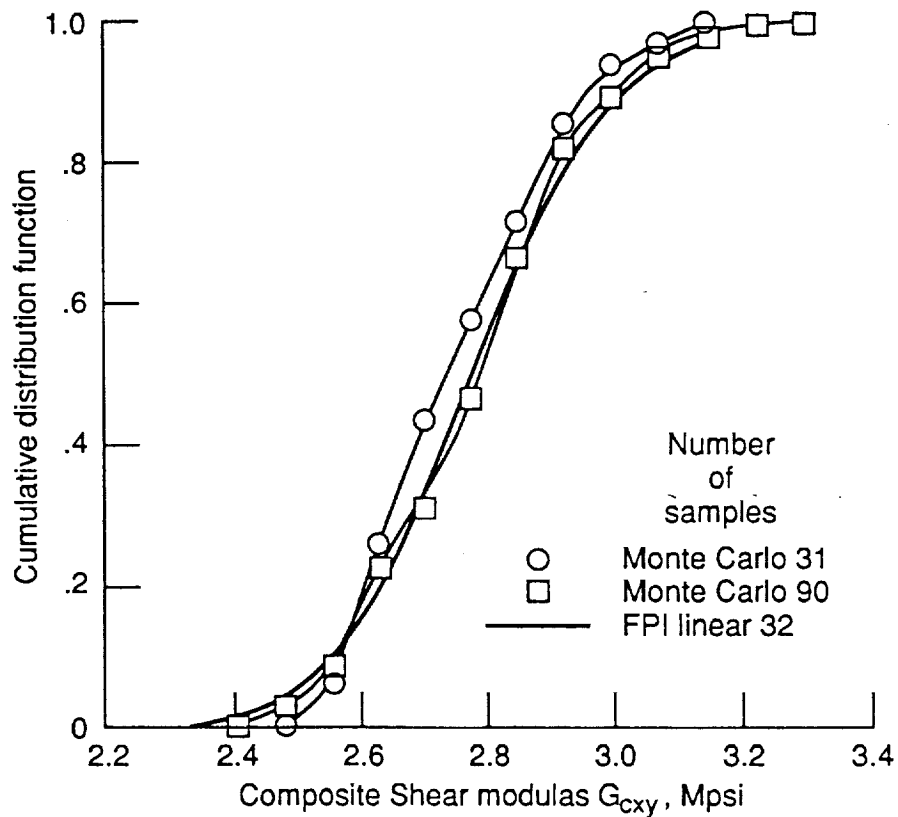


Figure 8. – Cumulative distribution function for composite $([0/45/90/-45]_s)$ Shear modulus G_{cxy} Simulation with Monte Carlo (no ply substructuring) and Fast Probability Integration (FPI).

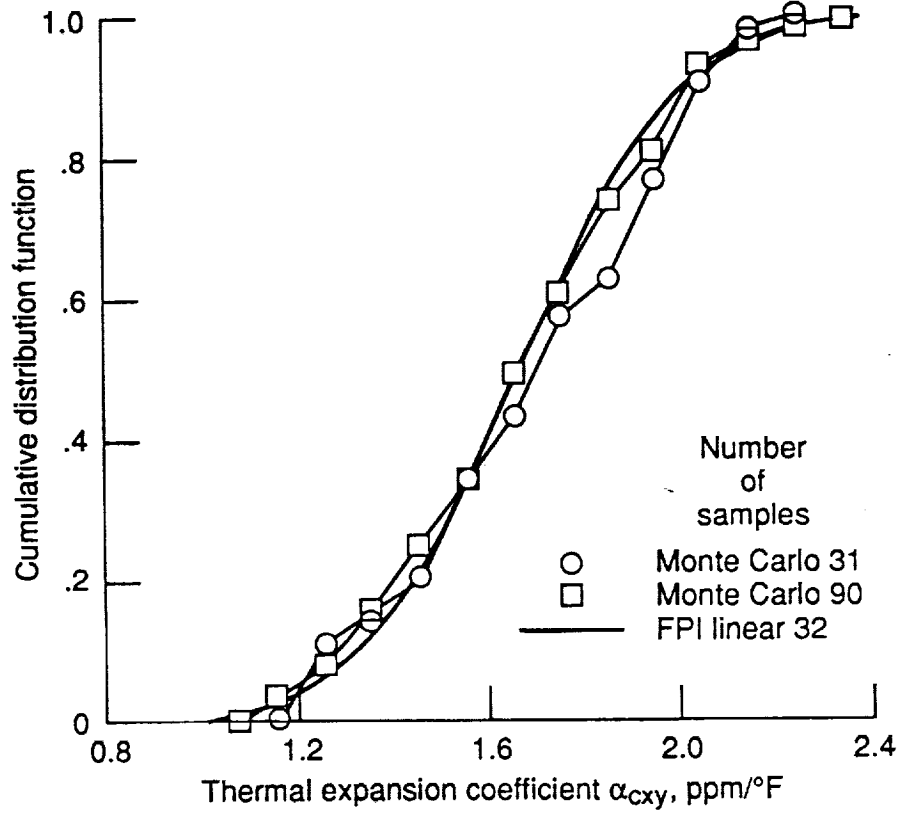


Figure 9. – Cumulative distribution functions for the composite ([0/45/90/-45]_s) thermal expansion coefficient α_{cxx} simulated with Monte Carlo (no ply substructuring) and Fast Probability Integration (FPI).

1. Report No. NASA TM-103669		2. Government Accession No.		3. Recipient's Catalog No.	
4. Title and Subtitle Probabilistic Micromechanics and Macromechanics of Polymer Matrix Composites				5. Report Date	
				6. Performing Organization Code	
7. Author(s) G.T. Mase, P.L.N. Murthy, and C.C. Chamis				8. Performing Organization Report No. E-5876	
				10. Work Unit No. 510-01-0A	
9. Performing Organization Name and Address National Aeronautics and Space Administration Lewis Research Center Cleveland, Ohio 44135-3191				11. Contract or Grant No.	
				13. Type of Report and Period Covered Technical Memorandum	
12. Sponsoring Agency Name and Address National Aeronautics and Space Administration Washington, D.C. 20546-0001				14. Sponsoring Agency Code	
15. Supplementary Notes Invited paper prepared for the 14th Annual Energy-sources Technology Conference and Exhibition sponsored by the American Society of Mechanical Engineers, Houston, Texas, January 20-24, 1991. G.T. Mase, GMI Engineering and Management Institute, Flint, Michigan 48504; P.L.N. Murthy and C.C. Chamis, NASA Lewis Research Center.					
16. Abstract A probabilistic evaluation of an eight-ply graphite/epoxy quasi-isotropic laminate was completed using the Integrated Composite Analyzer (ICAN) in conjunction with Monte Carlo simulation and Fast Probability Integration (FPI) techniques. Probabilistic input included fiber and matrix properties, fiber misalignment, fiber volume ratio, void volume ratio, ply thickness and ply layup angle. Cumulative distribution functions (CDFs) for select laminate properties are given. To reduce number of simulations, a Fast Probability Integration (FPI) technique was used to generate CDFs for the select properties in the absence of fiber misalignment. These CDFs were compared to a second Monte Carlo simulation done without fiber misalignment effects. It is found that FPI requires a substantially less number of simulations to obtain the cumulative distribution functions as opposed to Monte Carlo Simulation techniques. Furthermore, FPI provides valuable information regarding the sensitivities of composite properties to the constituent properties, fiber volume ratio and void volume ratio.					
17. Key Words (Suggested by Author(s)) Composites; Probabilistic mechanics; Micromechanics; Macromechanics; Composite mechanics; Laminate theory; Fast probability integrator; Monte Carlo simulation; Sensitivities; Properties				18. Distribution Statement Unclassified - Unlimited Subject Category 24	
19. Security Classif. (of this report) Unclassified		20. Security Classif. (of this page) Unclassified		21. No. of pages 19	
				22. Price* A03	

